YJCPH 1662
5 June 2007; Disk Used
ARTICLE IN PRESS
No. of Pages 23, Model 3+

Available online at www.sciencedirect.com
ScienceDirect
Journal of Computational Physics xxx (2007) xxx–xxx
JOURNAL OF COMPUTATIONAL PHYSICS
www.elsevier.com/locate/jcp

Progress in ocean wave forecasting

Peter A.E.M. Janssen *

European Centre for Medium-Range Weather Forecasts, Shinfield Park, Reading RG2 9AX, United Kingdom

Received 30 October 2006; received in revised form 10 April 2007; accepted 14 April 2007

Abstract

Progress in ocean wave forecasting is described in the context of the fundamental law for wave prediction: the energy balance equation. The energy balance equation gives the rate of change of the sea state caused by adiabatic processes such as advection, and by the physical source functions of the generation of ocean waves by wind, the dissipation due to white-capping and the nonlinear four-wave interactions. In this paper we discuss the formulation of the physics source functions and we discuss the numerical scheme that is used to solve the energy balance equation (with special emphasis on the so-called Garden-Sprinkler effect). Improvement in ocean wave forecasting skill is illustrated by comparing forecasts results with buoy observations for different years. Finally, the promising new development of the forecasting of extreme events is discussed as well.

Keywords: Energy balance equation; Wave forecasting; Wind input; Dissipation by white-capping; Four-wave interactions; Garden-Sprinkler effect

1. Introduction

In this paper, we would like to give a brief description of the developments in wave forecasting over the past 50 years, which is followed by a review of the experience with wave modelling at ECMWF. In the early 1960s there was a rapid development of the statistical theory of ocean waves, culminating in the basic evolution equation for the ocean wave spectrum: the *energy balance equation*. This equation tells us that the wave spectrum evolution is determined on the one hand by the adiabatic effects of advection and refraction, and, on the other hand by a source function S which is the sum of physical processes such as wind input, dissipation by wave breaking and nonlinear interactions. The energy balance equation has provided an appropriate framework for further wave model development as physical processes can be studied in isolation, and once understood, can be simply added to the source function S.

However, it is only 15 years ago that operational wave forecasting started using the complete energy balance equation, including an explicit representation of the physics of nonlinear interactions, wind input and

* Tel.: +44 118 949 9116; fax: +44 118 986 9450.
E-mail address: p.janssen@ecmwf.int.

0021-9991/$ - see front matter © 2007 Published by Elsevier Inc.
doi:10.1016/j.jcp.2007.04.029

dissipation. There are a number of reasons why it took such a long time before operational wave forecasting was done following this rational approach. First of all, in the early sixties the importance of the nonlinear interactions was not recognized and/or realized and researchers developed spectral wave models that only involved the effects of wave energy advection, wind input and a rudimentary form of dissipation by white-capping. Although these so-called *first-generation* models were applied successfully for many years, doubts have existed since their inception as to whether they really represented the physics of wave generation correctly. In order to reproduce the observed wave growth, the wind input source function had to be increased by almost an order of magnitude beyond the theoretical estimates of Jeffreys [1,2] and Miles [3]. The models were further unable to explain the pronounced overshoot phenomenon of a growing windsea[1] first observed by Barnett and Wilkerson [4] and subsequently confirmed by many other workers.

These problems were to some extent resolved in the early 1970s through extensive field measurements of wave growth under carefully selected, uniform fetch-limited wind conditions [5,6]. The analysis of these observations led to a different view of the energy balance of a growing windsea. According to the revised picture, the principle energy source during the growth phase of the waves on the low-frequency forward face of the spectrum was the nonlinear energy transfer from higher-frequency components to the right of the spectral peak, rather than direct wind forcing. The wind input source function on the forward face of the spectrum was nearly an order of magnitude smaller than that assumed in the first-generation models. This was therefore consistent both with earlier theoretical estimates and with later direct measurements of the work done by the pressure fluctuations on the moving wave surface by Snyder et al. [7] and Hasselmann and Bösenberg [8]. Apart from being responsible for the rapid growth rates on the forward face of the peak, the nonlinear transfer was also found to control the shape of the spectrum, including the development of the peak itself. In agreement with observations, the spectral peak of a growing windsea was found to be enhanced by about a factor of three relative to the form for a fully developed spectrum, which provided a natural explanation of the already mentioned overshoot phenomenon.

Therefore, in the mid seventies it was clear that nonlinear interactions had a profound impact on spectral evolution, but at the same time it was clear that because of lack of computing power it was not possible to include the effects of the nonlinear transfer directly in the energy balance equation. However, for growing windsea nonlinear interactions are fast compared to the other processes and since the nonlinear transfer controls spectral shape a universal, quasi-equilibrium spectral distribution is established which can be approximately characterized by a single, slowly changing scale parameter such as the total energy or the peak frequency. Thus, the so-called *second-generation* models emerged which were based on a parametric description of windsea (usually given by a JONSWAP spectrum [6]). The swell[2] component of the sea state is obtained from the energy balance in the absence of the source function S. 'Rules of thumb' are applied when a wave component has contributions from both windsea and swell.

Second-generation wave models have been applied with some success for many years, and some of them are still operational today. However, from the outset it became clear that for strongly nonuniform wind fields (e.g. near fronts, intense tropical cyclones or midlatitude storms), the advective terms are able to compete with the nonlinear energy distribution, and significant deviations from the quasi-equilibrium spectral distribution may occur. The SWAMP study [9] compared the results of nine different first and second-generation models in simple, hypothetical conditions and, in particular for a hurricane wind field it was found that the models behaved quite differently. For example, the maximum significant wave height ranged between 8 and 25 m, reflecting our lack of knowledge at that time. In particular, the equilibrium ideas of the second-generation models combined with the 'rules' of thumb did not always seem to work. In rapidly varying circumstances an explicit representation of the nonlinear interactions was required.

In the 1980s the introduction of the first supercomputers and the promise of the wealth of data on the ocean surface from remote-sensing instruments on board of new satellites such as ERS-1 and Topex-Poseidon provided a significant stimulus to the development of a new generation of ocean wave prediction models. In other

[1] Windsea is that part of the sea state that is subject to wind forcing. These forced wind waves are usually steep and therefore, apart from wind input, nonlinear processes such as four-wave interactions and dissipation by white-capping determine the shape of the spectrum.

[2] Swell is that part of the sea state that is not subjected to wind forcing. Swell can be considered as almost linear and because the waves are long there is hardly any dissipation, hence these waves may propagate over large distances, of the order of an ocean basin.

Please cite this article in press as: P.A.E.M. Janssen, Progress in ocean wave forecasting, J. Comput. Phys. (2007), doi:10.1016/j.jcp.2007.04.029

words, the time seemed ripe for the development of a *third-generation* model, i.e. a full spectral model with an explicit representation of the physical processes relevant for wave evolution, giving a full two-dimensional description of the sea state. However, before an operational model could be developed, a number of hurdles needed to be overcome. First, it was important to establish that for simple hypothetical cases such a third-generation wave prediction gave a realistic description of the sea state. Evidence for the simple duration limited case was provided by Komen et al. [10], who showed that with a plausible representation of the wind input and dissipation source function together with an explicit representation of the nonlinear interactions a realistic steady-state solution (closely resembling the empirical Pierson–Moskowitz spectrum [11]) could be achieved. Second, even with present-day computing power a wave prediction model based on the exact presentation of the nonlinear interactions is not feasible. Some form of parametrization on the nonlinear transfer is required and was provided by Hasselmann et al. [12] who introduced an operator parametrization called the 'discrete interaction approximation' (DIA). The DIA is efficient, and it takes care in a realistic manner of two important properties of the nonlinear transfer, namely the downshift of the peak of the spectrum and the formation of a quasi-equilibrium spectrum.

These important findings combined with the availability of sufficient computing power paved the way for a rapid development of the third-generation WAve Model (WAM). The WAM group was formed at the end of 1984 and a few years later already a number of promising achievements were reported in WAMDI [13]. Importantly, the WAM model was capable to produce realistic wave spectra in case of the rapidly varying circumstances of hurricane Camille. Because of these promising results, over the past 15 years most of developments in operational wave forecasting have taken place in the context of third-generation wave models. The wave model community has become a very active field. During this period, apart from the WAM model [14], several new models have been introduced. For example, there is a wave model with alternative formulations for the physics of wind input and dissipation (WaveWatch III [15]), there is a wave model with an alternative formulation of the DIA (MRI-III [16]), and there is a wave model that concentrates on the physics of waves in the coastal zone (SWAN [17]). Having most experience with the workings of the WAM model we will concentrate on the results obtained with this model.

The present paper does *not* represent a consensus view of the main developments and achievements in the field of ocean wave forecasting. The opinions of the researchers in the ocean wave community are diverse. Perhaps there is a consensus that the fundamental law of wave prediction is the energy balance equation, but how well the physics of wind input, dissipation and nonlinear interactions is understood is a subject of heated debates. An innocent bystander would perhaps wonder whether, given these large uncertainties in our knowledge of wave dynamics, it is at all possible to have a viable operational wave forecasting system. The thrust of this paper is that this is indeed possible and in fact we have seen considerable improvements in wave forecasting skill over the past 15 years. Here, improvements will be measured by validating WAM model forecast results against observations of the sea state.

The present paper is organized as follows: in Section 2 a discussion is given of the basic evolution equation for the ocean wave spectrum, known as the energy balance equation, the transport equation or the radiative transfer equation. After a brief discussion of the formulation of the physics source functions, it is shown that in case of the generation of ocean waves by wind, the solution of the energy balance has a number of desirable properties: the ocean wave spectrum shows a considerable downshifting of the peak of the spectrum which corresponds to a sea state that gradually gets more and more coherent. In addition, the simulation shows a pronounced overshoot of wave energy near the peak of the spectrum. In Section 3 we discuss some of the details of the numerical scheme used in the solution of the energy balance equation. In particular, we discuss the so-called 'Garden-Sprinkler effect' which occurs because of the finite resolution of the wave spectrum in frequency and direction. To a considerable extent the quality of wave prediction results depends on the accuracy of the forcing wind fields. In order to illustrate this we show in Section 4 the verification of forecast wind and wave results against buoy data over the past 15 years. Therefore, wave results are of great help in diagnosing problems in atmospheric models. In Section 5 we discuss a new development. The last few years there has been a considerable interest in trying to understand under what conditions extreme sea states (usually connected with 'freak' waves) occur. The question now is to what extent statements on the occurrence of extreme states can be made realizing that the energy balance equation describes the evolution of the average sea state. The average sea state has in lowest order a Gaussian probability distribution function (pdf) for the surface

Please cite this article in press as: P.A.E.M. Janssen, Progress in ocean wave forecasting, J. Comput. Phys. (2007), doi:10.1016/j.jcp.2007.04.029

elevation, corresponding to linear waves. Finite amplitude effects result in deviations from Normality and for weakly nonlinear waves these deviations in the pdf can be calculated and result in valuable information on extreme sea states.

2. The laws of wave prediction

Interest in wave prediction started during the Second World War because of the practical need for knowledge of the sea state during landing operations. The first operational predictions were based on the work of Sverdrup and Munk [18], who introduced a parametrical description of the sea state and who used empirical windsea and swell laws. Manual techniques based on this approach have been used by operational forecasters for many years and these techniques turned out to be a convenient means to obtain for a given wind field a short term forecast [19]. In the mean time, an important advance was the introduction of the concept of a wave spectrum [20], while the corresponding dynamical evolution equation, the energy balance equation, was proposed by Gelci et al. [21]. The wave spectrum at a certain location describes the average sea state in a finite area around that location. It only gives information on the energy distribution of the waves and not of the phase of the individual waves. Note that in practice observations of the phase of the waves are not available anyway, so we have to content ourselves with an averaged description of the sea state. For most practical purposes this turns out to be sufficient.

On the open ocean surface gravity waves can to first approximation be regarded as linear. Thus, in agreement with many linear wave phenomena, the kinetic energy of a surface gravity wave equals the potential energy, hence the total energy E of a wave is given by twice the potential energy. With η the surface elevation, ρ_w the water density and g acceleration of gravity, the energy of a linear wave becomes

$$E = \rho_w g \eta^2 \tag{1}$$

Since for our practical purposes water density and acceleration of gravity may be regarded as constant we concentrate on the variance of the surface elevation η^2, which is a function of space and time. In particular, we are therefore interested in the spectrum corresponding to the surface elevation, i.e. we need to know the evolution of the wave variance spectrum (from now on we simply refer to it as the spectrum).

Let us denote the wave number spectrum by $F(\mathbf{k};\mathbf{x},t)$. It gives the distribution of wave variance over wavenumber $\mathbf{k}$. In addition, it is assumed that the wave spectrum is a slowly varying function of position $\mathbf{x}$ and time t. Here, slow has a relative meaning; it refers to the basic length and time scale imposed by the waves, namely their typical wavelength and period. Thus, the spectrum is supposed to vary slowly in space and time compared to the basic wave length and period of the waves (in physics this is usually referred to as the geometrical optics approximation). In slowly varying circumstances, as induced by varying environmental conditions caused by currents $\mathbf{U}(\mathbf{x},t)$ and depth $D(\mathbf{x})$, it is well known [22] that wave action is an adiabatic invariant, and not wave energy. Therefore, in wave forecasting the fundamental quantity to predict is the action density spectrum $N(\mathbf{k};\mathbf{x},t)$. It is defined as

$$N = \frac{gF}{\sigma} \tag{2}$$

with $\sigma = \sqrt{gk\tanh(kD)}$ the intrinsic angular frequency. The action density plays the role of a number density of waves, hence, apart from the 'constant' water density ρ_w, the energy E of the waves is given by $E = \sigma N$, while the wave momentum $\mathbf{P}$ is given by $\mathbf{P} = \mathbf{k}N$.

For surface gravity waves evolving on a slowly varying current $\mathbf{U}$ in an ocean basin with slowly varying depth D, the energy balance equation is given by

$$\frac{\partial N}{\partial t} + \cdot\nabla_{\mathbf{x}} \cdot (\nabla_{\mathbf{k}}\Omega N) - \nabla_{\mathbf{k}} \cdot (\nabla_{\mathbf{x}}\Omega N) = S. \tag{3}$$

Here, Ω represents the dispersion relation

$$\Omega = \mathbf{k}\cdot\mathbf{U} + \sigma, \tag{4}$$

and S on the right-hand side of Eq. (3) is the source function. Although there is consensus among the wave community in Eq. (3), there are quite diverse views about the exact representation of S. The most widely ac-

Please cite this article in press as: P.A.E.M. Janssen, Progress in ocean wave forecasting, J. Comput. Phys. (2007), doi:10.1016/j.jcp.2007.04.029

cepted view suggests that S represents the physics of wind-wave generation ($S_{\rm in}$), dissipation by wave breaking and other causes ($S_{\rm dissip}$) and four-wave interactions ($S_{\rm nonlin}$). In other words,

$$S = S_{\rm in} + S_{\rm nonlin} + S_{\rm dissip}. \tag{5}$$

Let us comment briefly how the energy balance equation is obtained. Consider first the case that there are no sources and sinks, hence $S = 0$. In this ideal case, surface gravity waves are a Hamiltonian system [23,24] and the equations of motion follow from a variational principle which minimizes the surface pressure. A straightforward application of Whitham's average variational principle then results (see e.g. [25,26]) in the vanishing of the left-hand side of the energy balance equation (called the adiabatic part). Therefore, in the absence of sources and sinks there are only two reasons why the wave spectrum changes in time, namely due to advection and due to refraction. There are, however, many other causes why the sea state may change with time. For example, waves grow because of the energy and momentum input by wind and they loose energy because of white-capping. In addition, finite steepness waves may interact nonlinearly with other waves in such a way that energy and momentum is conserved. As long as these perturbations are small they can be added because products of the effects of, for example, wind input and nonlinear transfer can safely be ignored. Hence, the source function S is the sum of a number of physical processes.

In the 1980s there was a major effort to develop realistic parametrisations of all the source functions. The present version of the WAM model has an input source function which is based on Miles critical layer mechanism [3] (including the feedback of the wave stress on the wind profile [27]), the nonlinear interactions are represented by means of the direct-interaction approximation (DIA) of Hasselmann et al. [12] while the dissipation source function is based on the work of Hasselmann [28]. A first account of this is given by [14], while a more up to date account of the status of wave modelling can be found in [26].

2.1. Wind input

Regarding the subject of the generation of surface waves by wind there has always be a strong interplay between theory and experiment. Because it is such a difficult problem this has led to many debates, controversy and confusion. From the theoretical point of view it should be realized that one is dealing with an extremely difficult problem because it involves a turbulent airflow over a surface that varies in space and time. Although there has been much progress in understanding turbulence over a flat plate in steady-state conditions, attempts to understand turbulent flow over (nonlinear) gravity waves are only beginning and there is still a considerable uncertainty regarding the validity of turbulence models in unsteady circumstances. Only recently, direct numerical simulations of the problem of wind wave growth for reasonable Reynolds numbers have been reported [29].

From an experimental point of view it should be pointed out that it is not an easy task to measure growth rates of waves by wind. First of all, one cannot simply measure growth rates by studying time series of the surface elevation since the time evolution of ocean waves is determined by a number of processes such as wind input, nonlinear interactions and dissipation. In order to measure the growth of waves by wind one therefore has to make certain assumptions regarding the process that causes wave growth. The commonly adopted cause of wave growth is the work done by the pressure on the surface. This assumption seems plausible in view of the work by Miles [3]. Secondly, because of the small air–water density ratio the growth rates are small which means that a very accurate determination of amplitude and phase of the wave-induced pressure fluctuations is required.

Nevertheless, considerable progress has been made over the past 50 years. The main mechanism for wave growth was suggested by Miles [3] who considered the simplified problem where effects of turbulence on the gravity wave motion was ignored. Note, however, that some researchers regard the neglect of turbulence a serious omission, so they have proposed alternative formulations of the wind input source function (see e.g. [15]). In that case there is in the air a critical height, defined by the condition that the phase speed of the surface gravity wave c matches the wind speed $U = U_0(z)$ (where z is the height above the sea surface), and this gives the possibility of a resonant momentum transfer between mean air flow and a particular gravity wave. In fact, it turns out that the growth rate of the waves by wind is proportional to the curvature in the wind profile at the critical height. The wind input source function becomes of the form

Please cite this article in press as: P.A.E.M. Janssen, Progress in ocean wave forecasting, J. Comput. Phys. (2007), doi:10.1016/j.jcp.2007.04.029

$$S_{\rm in} = \gamma N \tag{6}$$

where γ is the growth rate of the energy of the waves which is given by

$$\gamma = \epsilon\omega\beta(u_*/c)^2\cos^2(\theta-\phi), \quad |\theta-\phi| < \pi/2. \tag{7}$$

Here, $\omega = \Omega$ is the angular frequency, ϵ the air–water density ratio, which is a small number typically of the order of 10^{-3}, and β is the so-called Miles parameter.[3] In Eq. (7) the strength of the wind is expressed in terms of the friction velocity $u_* = \tau^{1/2}$ where the kinematic stress τ gives the total loss of momentum from air to water. Finally, θ is the direction in which the waves propagate and ϕ is the wind direction.

According to the dispersion relation short gravity waves have a lower phase speed than long gravity waves, and as a consequence from Eq. (7) it follows that short waves grow the fastest. In addition, according to Eq. (7) only those waves are affected by wind that have a phase speed with a component in the wind direction. Possible small damping effects for waves propagating against the wind are ignored by this formulation.

The growth rate is found to be proportional to the total stress τ. Now, part of the total stress, called the wave-induced stress $\tau_{\rm w}$, is caused by the momentum transfer from the air to the waves, while the remainder is due to the slowing down of the air by turbulent transport ($\tau_{\rm t}$) and viscosity ($\tau_{\rm v}$). In other words,

$$\tau = \tau_{\rm w} + \tau_{\rm t} + \tau_{\rm v}. \tag{8}$$

Here, the wave-induced stress is simply given by the rate of change in time of the wave momentum due to wind, or,

$$\tau_{\rm w} = \int {\rm d}\mathbf{k}\mathbf{k}\frac{\partial}{\partial t}N\bigg|_{\rm wind} = \int {\rm d}\mathbf{k}\,\mathbf{k}S_{\rm in} \tag{9}$$

where $S_{\rm in}$ is given by Eqs. (6) and (7). Therefore, the total stress depends on the rate of change of the sea state, and, since the growthrate depends on the total stress a definite answer for the growthrate of the wind waves can only be obtained by iteration. In other words, there is a mutual two-way interaction between wind and waves, and for this reason ECMWF runs, since June 1998, a coupled weather–ocean wave forecasting system. More details regarding the theory of wind-wave interaction can be found in [26] where also the impact of the sea state dependent momentum transfer on weather and wave forecasting is discussed.

Miles' theory of wind-wave generation has been criticized in the past for being simplistic, as for example effects of turbulence on the wave-induced motion in the air were disregarded. Recently, evidence in favour of the critical layer approach was presented in literature. First, Sullivan et al. [29] studied the growth of waves by wind in the context of an eddy-resolving numerical model. Although the Reynolds number was, compared to nature, too small by an order of magnitude, clear evidence for the existence of a critical layer was found for a wide range of dimensionless phase speeds. As expected from the Miles mechanism, a rapid fall-off of the wave-induced stress was seen at the critical layer. Furthermore, nowadays, there is even direct evidence of the existence and relevance of the critical layer mechanism from in situ observations [30] obtained from FLIP (a floating instrument platform created by two Scripps scientists some 40 years ago). This is quite a challenge because one has to extract a relatively small wave-coherent signal from a noisy signal. Nevertheless, for the range $16 < c/u_* < 40$, Hristov et al. [30] could see a pronounced cat's-eye pattern around the critical height where the wave-induced stress showed a jump. There was good agreement between observed and modelled wave-induced profiles. Note that it is not clear from observations whether there is a critical layer for dimensionless phase speeds less than 16. These conditions can only be observed when measurements are taken close enough to the ocean surface, in between the ocean waves.

As already pointed out, the momentum transfer from the air to the waves may be a function of the sea state itself, so that a strong coupling between the turbulent boundary layer and the surface waves is expected. Observations confirm this expectation. Measurements from dedicated field campaigns reported in, for example [31–34] indicate that the momentum transfer is sea-state dependent and that it therefore makes sense to tightly couple a weather forecasting model and a wave forecasting model. However, Miles theory and the idea of two-way interaction have only been validated for fairly moderate wind speeds, say up to 20 m/s. For really strong

[3] The parameter β follows from an eigenvalue problem for the wave-induced velocity in the air, and is for short waves fairly constant.

Please cite this article in press as: P.A.E.M. Janssen, Progress in ocean wave forecasting, J. Comput. Phys. (2007), doi:10.1016/j.jcp.2007.04.029

wind cases, such as occur in hurricanes, one enters a new regime. In those cases the ocean surface is, because of very frequent breaking waves, not well defined. The associated spray production may play an important role because a very stable layer of 'air' is formed close to the surface which may suppress the air turbulence. Other effects, such as air-flow separation may play a role as well. Clearly, it is not easy to obtain reliable observations in these circumstances and because of all these complications wave growth by wind and the associated momentum transfer for strong winds is still an active area of research.

2.2. Nonlinear four-wave interactions

Ocean waves may be regarded most of the time as weakly nonlinear, dispersive waves. Because of this there is a small parameter present which permits to study the effect of nonlinearity on wave evolution by means of a perturbation expansion with starting point linear, freely propagating ocean waves. In addition, it should be pointed out that the subject of nonlinear ocean waves has conceptually much in common with nonlinear wave phenomena arising in diverse fields such as optics and plasma physics. In particular, since the beginning of the 1960s many people have contributed to a better understanding of the properties of nonlinear waves, and because of the common denominator we have seen a relatively rapid progress in the field of nonlinear ocean waves.

In fact, the study of nonlinear effects on deep-water gravity waves started in the 19th century with the important contribution of Stokes [35]. He considered a single wave of permanent shape and was able to find the effects of finite amplitude on the dispersion relation by means of a so-called singular perturbation technique. In hindsight, he may be regarded as the 'father' of the renormalization technique – nowadays so popular in particle physics – because he found the dispersion relation of finite amplitude gravity waves by renormalization of the acceleration of gravity g. Later, Levi-Civita [36] proved the convergence of the Stokes series solution.

In 1965, Lighthill [37] discovered, using Whitham's variational approach, that a nonlinear, deep-water gravity wave train is unstable to modulational perturbations, giving rise to a deeply modulated wave train, hence focussing wave energy in space and time, and as a consequence the growth of sidebands in the corresponding spectrum. This instability may be regarded as a special case of a four-wave interaction process, which, as we will see, plays an important role in the physics of ocean waves. In the field of fluid dynamics this instability is nowadays known as the Benjamin–Feir instability, because Benjamin and Feir [38] were the first to give experimental evidence of its existence. In other fields it is referred to as the modulational instability or sideband instability.

Wave forecasting is about a description of the average sea state. As already discussed, one is then interested in a statistical description of the sea surface, which means one is concerned with the evolution of the energy of an ensemble of waves. Although for extreme events, such as occur in the presence of freak waves, there is a need for information on the phases of the waves it is noted that the prediction of the phase of the individual waves is a hopeless adventure. First, we have no observations of the initial phases of the waves, and, second, long-time integrations of the deterministic evolution equations exhibit features of chaotic behaviour [39]. In other words, after a finite time the phases of the waves will show a very sensitive dependence on the initial conditions, and therefore in practice they are not predictable.

Let us briefly describe how to obtain from the deterministic evolution equations an equation for the ensemble averaged wave spectrum. Introduce the Fourier transform $\hat{\eta}$ of the surface elevation η

$$\eta(\mathbf{x},t) = \int \mathrm{d}\mathbf{k}\,\hat{\eta}(\mathbf{k},t)\mathrm{e}^{\mathrm{i}\mathbf{k}\cdot\mathbf{x}} \tag{10}$$

As the action is the basic variable for waves we transform to action variables $a(\mathbf{k})$

$$\hat{\eta}(\mathbf{k}) = \left(\frac{k}{2\omega}\right)^{1/2}[a(\mathbf{k}) + a^*(-\mathbf{k})]. \tag{11}$$

This is then substituted in the Hamilton equations of motion, and, when truncated to third-order in amplitude, results in a nonlinear set of equations for the action variable a, which is known as the Zakharov equation [24]. The general form of this equation is

Please cite this article in press as: P.A.E.M. Janssen, Progress in ocean wave forecasting, J. Comput. Phys. (2007), doi:10.1016/j.jcp.2007.04.029

$$\frac{\partial a_1}{\partial t} + i\omega_1 a_1 = -\mathrm{i}\int \mathrm{d}\mathbf{k}_{2,3,4} T_{1,2,3,4} a_2^* a_3 a_4 \delta_{1+2-3-4}, \tag{12}$$

where we have introduced the short hand notation $a_1 = a_1(\mathbf{k}_1)$, $\mathrm{d}\mathbf{k}_{2,3,4} = \mathrm{d}\mathbf{k}_2\mathrm{d}\mathbf{k}_3\mathbf{k}_3$, $\delta_{1+2-3-4} = \delta(\mathbf{k}_1 + \mathbf{k}_2 - \mathbf{k}_3 - \mathbf{k}_4)$, etc. The interaction coefficient $T_{1,2,3,4}$ is given by Krasitskii [40]. The interaction coefficient enjoys a number of symmetry conditions, of which the most important one is $T_{1,2,3,4} = T_{3,4,1,2}$, because this condition implies that the evolution equation is Hamiltonian.

The Zakharov equation tells us that the amplitude a_1 only changes when one can find three other waves in such a way that the resonance condition in wavenumber space, $\mathbf{k}_1 + \mathbf{k}_2 - \mathbf{k}_3 - \mathbf{k}_4 = 0$, is satisfied. Hence, it is a 'classical' form of a four-wave interaction process. Nowadays, many properties of Eq. (12) have been studied, and it turns out that this equation gives a fair description of the stability properties of surface gravity waves both in deep water [41] and in shallow water [42]. It is therefore a good starting point for a statistical description of the sea state.

For a homogeneous sea,[4] the action density spectrum $N(\mathbf{k})$ is now related to the second moment $\langle a_1 a_2^* \rangle$ in the following fashion

$$\langle a_1 a_2^* \rangle = N(\mathbf{k}_1)\delta(\mathbf{k}_1 - \mathbf{k}_2), \tag{13}$$

where the angle brackets denote an ensemble average. The equation for the second moment now follows by differentiating $\langle a_1 a_2^* \rangle$ with respect of time and by applying the Zakharov equation to eliminate the time derivatives of a_1 and a_2^*. Because of nonlinearity the evolution of the second moment involves the fourth moment, and, similarly the equation for the fourth moment involves the sixth moment. In this way an infinite hierarchy of equations is found, and in order to close the hierarchy additional assumptions need to be made. Hasselmann [43] argued convincingly that for ocean waves it is appropriate to make the assumption of a near-Gaussian, homogeneous wave field (also known as the Random Phase Approximation). For a Gaussian sea state higher order moments may be expressed in terms of the second moment, thus achieving closure of the hierarchy. The resulting evolution equation becomes

$$\frac{\partial}{\partial t} N_1 = 4\pi \int \mathrm{d}\mathbf{k}_{2,3,4} |T_{1,2,3,4}|^2 \Delta_{1+2-3-4} [N_3 N_4 (N_1 + N_2) - N_1 N_2 (N_3 + N_4)], \tag{14}$$

where we introduced the abbreviation $\Delta_{1+2-3-4} = \delta_{1+2-3-4}\delta(\omega_1 + \omega_2 - \omega_3 - \omega_4)$. For gravity waves this evolution equation was first obtained by Hasselmann [43] and we will refer from now to it as the Hasselmann equation. Accordingly, the action density is seen to change in time owing to *resonant* four-wave interactions only, where the resonance conditions follow from the vanishing of the arguments of the Dirac δ-functions: $\omega_1 + \omega_2 = \omega_3 + \omega_4$, and $\mathbf{k}_1 + \mathbf{k}_2 = \mathbf{k}_3 + \mathbf{k}_4$.

The Hasselmann equation has the desirable property that the action density, being a positive quantity, remains positive for all time. Furthermore, the two scalar quantities total action and energy and one vector quantity wave momentum are conserved by the resonant four wave interactions. Finally, there is a principle of detailed balance as action momentum and energy are conserved for each resonant interaction quadruplet separately.

The evaluation of the exact expression of the nonlinear transfer is, however, time consuming, and even with present-day computing power it is operationally not feasible to evaluate the nonlinear interactions on a global scale (A typical global application of a wave prediction system has of the order 10^5 number of gridpoints, while the wave spectrum has 30 frequencies and 24 directions). Therefore, a parametrization of this nonlinear effect is required. To date, the most successful attempt is the work of Hasselmann et al. [12] who introduced the DIA. Essentially, guided by the principle of detailed balance, the nonlinear energy transfer is determined for each wave component by choosing one representative quadruplet (and its mirror image). Of course, there is still active research on obtaining a more accurate approximation to the nonlinear four-wave interactions, but the DIA is nowadays still used by the majority of third-generation wave models.

[4] A seastate is regarded as homogeneous when the spatial correlation function only depends on the distance between the two points of interest.

Please cite this article in press as: P.A.E.M. Janssen, Progress in ocean wave forecasting, J. Comput. Phys. (2007), doi:10.1016/j.jcp.2007.04.029

To what extent is there experimental evidence for the nonlinear transfer for surface gravity waves. To our knowledge there is no direct evidence in the field for the resonant transfer because nonlinear interaction is a fast process that cannot be isolated from the action of wind input and dissipation. In the laboratory, the four-wave interaction process can be studied in isolation and for particular choices of the wavenumbers McGoldrick et al. [44] carried out a series of careful measurements which revealed the existence of resonant interaction in agreement with the analytical results obtained by Phillips [45]. Another example is the Benjamin–Feir instability which is a degenerate case of four-wave interaction, where $\mathbf{k}_1 = \mathbf{k}_2$ is given by the carrier wavenumber $\mathbf{k}_0$, while the wavenumbers $\mathbf{k}_3$ and $\mathbf{k}_4$ are given by the sideband wavenumbers $\mathbf{k}_0(1 \pm \epsilon)$ which need to be sufficiently close to the carrier wavenumber in order to get instability. There is also evidence from numerical simulations that supports Hasselmann's theory. Tanaka [46] simulated the evolution of a continuous spectrum using the Hamilton equations in two-dimension truncated to third order in amplitude and satisfactory agreement was obtained, while Janssen [47] did Monte Carlo simulations with the one-dimensional version of the Zakharov equation and found good agreement with Hasselmann's theory provided the effects of near-resonant interactions were taken into account as well.

2.3. Dissipation

Waves may loose energy continuously by viscous dissipation and by the highly intermittent process of wave breaking. In addition, the (small-scale) breaking waves generate eddies in the surface layer of the ocean. These eddies may give rise to damping of the longer ocean waves. Furthermore, ocean waves may loose energy because of the generation of organized motions in the ocean such as Langmuir circulations and in the presence of a vertical shear in the current.

Understanding and modelling of the wave breaking process is of importance in achieving an accurate representation of the principal sink in the action balance equation. Unfortunately, even nowadays there has not been much progress in obtaining a convincing model of dissipation caused by wave breaking or white-capping. This should not come as a surprise, because wave breaking is a truly nonlinear phenomenon that cannot be captured by the usual perturbation techniques. A straightforward theoretical approach seems therefore not possible. Although there has been considerable progress in the numerical modelling of breaking of individual waves, it is hard to see how these results may be extended to the general case of a random wave field.

Nevertheless, there has been progress in modelling dissipation by whitecaps in a semi-empirical manner. The most prominent approach is from Hasselmann [28]. The assumptions behind Hasselmann's white cap model are that the white caps can be treated as a random distribution of perturbations, which are formally equivalent to pressure pulses, and that the scales of the white caps in space and time are small compared to the scales of the associated wave. The theoretical development consists of two steps. First, it is shown that all processes that are weak-in-the-mean, even if they are strongly nonlinear locally, yield source functions which are quasi-linear in lowest approximation. The source function consists of the spectrum at the wavenumber considered multiplied by a factor which is a functional of the entire wave spectrum. Introducing the zeroth moment of the wave spectrum F,[5]:

$$m_0 = \int \mathrm{d}\mathbf{k} F(\mathbf{k}) \tag{15}$$

the mean frequency $\langle\omega\rangle$ is defined as

$$\langle\omega\rangle = \int \mathrm{d}\mathbf{k}\omega F(\mathbf{k})/m_0 \tag{16}$$

and using a similar relation for the mean wavenumber $\langle k\rangle$, the final result is the following dissipation source function

[5] Note that a statistical measure of the wave height, called the significant wave height H_S, is directly obtained from the zeroth moment as $H_S = 4(m_0)^{1/2}$. This parameter is of primary concern in wave forecasting.

Please cite this article in press as: P.A.E.M. Janssen, Progress in ocean wave forecasting, J. Comput. Phys. (2007), doi:10.1016/j.jcp.2007.04.029

$$S_{ds} = -\gamma_d N, \tag{17}$$

with

$$\gamma_d = \beta\langle\omega\rangle(\langle k\rangle^2 m_0)^m\left[\frac{k}{\langle k\rangle} + a\left(\frac{k}{\langle k\rangle}\right)^2 + \ldots\right], \tag{18}$$

where in accordance with one's intuition the dissipation increases with increasing steepness parameter $\langle k\rangle^2 m_0$. Here, β, a and m are unknown constants which are determined in such a way that the observed spectral evolution (e.g. from JONSWAP [6]) is reproduced. The first rationale attempt to determine the unknown coefficients in the dissipation source function was reported in [10]. They started from the empirical expression for wind input of Snyder et al. [7], which was adapted to accommodate friction velocity scaling, whilst the exact form of Hasselmann's nonlinear transfer was taken. For a constant wind speed, the energy balance equation was integrated until stationary conditions were reached, and the unknown coefficients m and β were chosen in such a way that the equilibrium spectrum resembled the Pierson–Moskovitz [11] spectrum as closely as possible (note that in their work a was put to zero from the outset). The power m was found to be equal to 2 while the coefficient β was of the order of 3.

Evidence for or against the dissipation source function (17) is hard to find, mainly because in the field it is difficult to study the dissipation process in isolation. Young and Babanin [48] studied an extreme shallow water case where more than 50% of the waves were breaking, and they found that indeed the dissipation is linear in the spectrum. Similarly, in another extreme case of wave propagation over an immersed bar, Battjes and Janssen [49] found that once the waves passed the bar there was a considerable breaking and the change of the spectrum was linear in the spectrum. Furthermore, using the dissipation source function it is possible to determine the whitecap fraction at the sea surface, a parameter which is easily detectable using a video camara. The modelled whitecap fraction turns out to be proportional to the steepness factor $(\langle k\rangle^2 m_0)^m$ thus providing an independent check on the magnitude of the power m by comparison with field data. A number of independent field campaigns [50,51] give a value for m of the order 2.

To summarize the discussion on the source functions it is mentioned that in the field of ocean wave forecasting the nonlinear transfer is regarded to be well known because it is based on a well-established approach. However, apart from numerical simulations, there is relatively little direct observational evidence on the importance of nonlinear interactions in the field. The wind input source function is relatively well known as well, because it compares favourably with field evidence of the rate of change of the wave spectrum by wind. The least known source function is the dissipation and in practice the parameters of the dissipation source function are tuned in such a way that the solution of the energy balance equation reproduces the observed evolution of the wave spectrum.

2.4. Energy balance for growing wind waves

In this section we discuss the solution of the energy balance equation for the simple case of the generation of ocean waves by wind. To that end we will study the idealized situation of duration-limited wave growth (when a uniform and steady wind has blown over an unlimited ocean for time t after a sudden onset and starting from a flat, calm sea). The case of an unlimited ocean follows when the advection terms in the energy balance equation are switched off so that one can simulate the duration-limited case by means of a single grid point version of the model. In this fashion we manage to concentrate on the properties of the source functions of the energy balance equation.

Although from a theoretical point of view it is most natural to discuss the evolution of gravity waves in terms of the action density, in practice one observes the surface elevation spectrum $F(f,\theta)$ where f is the frequency of the waves (it follows from the definition $\omega = 2\pi f$) and theta is the propagation direction. The relation between action density and frequency spectrum follows from Eq. (2) which is a relation in terms of wavenumber spectral densities. The conversion of wavenumber to frequency is achieved by making use of the dispersion relation, and the condition that energy is conserved during the transformation. The result is

$$F(f,\theta) = \sigma N(f,\theta)/g, \tag{19}$$

Please cite this article in press as: P.A.E.M. Janssen, Progress in ocean wave forecasting, J. Comput. Phys. (2007), doi:10.1016/j.jcp.2007.04.029

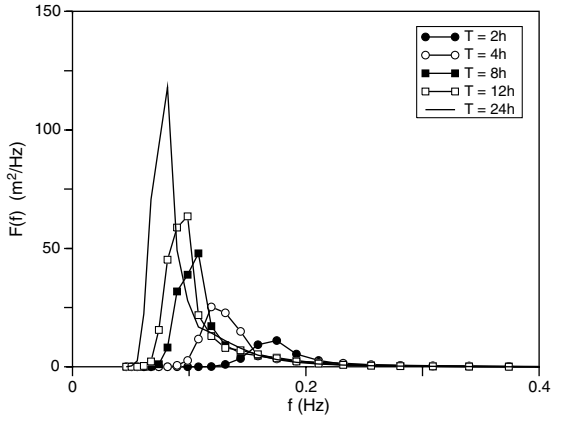

Fig. 1. Evolution in time of the one-dimensional frequency spectrum according to the ECWAM model.

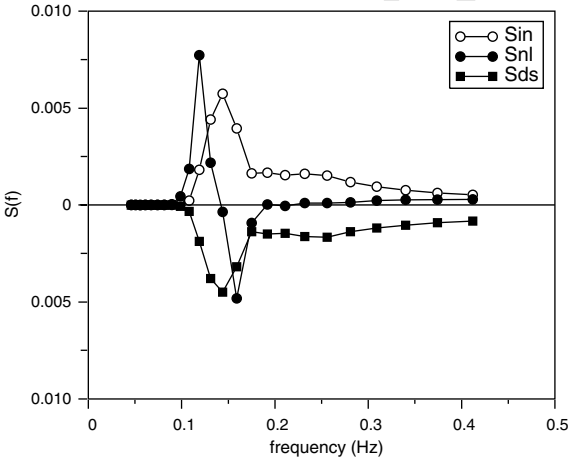

Fig. 2. The energy balance for young windsea at a duration of 4 h.

with σ the intrinsic frequency, and wave prediction models such as the WAM model have been formulated in terms of the frequency-direction spectrum $F(f,\theta)$. In the numerical model, the continuous spectrum is approximated by step functions that are constant in a frequency-direction bin. Present-day wave forecasting systems have typically $N_{\mathrm{ang}} = 24$ directions and $N_{\mathrm{fre}} = 30$ frequencies, hence per grid point we deal with 720 equations. The frequencies are on a logarithmic scale, with a relative frequency increment $\Delta f/f = 0.1$, spanning a frequency range $f_{\max}/f_{\min} = (1.1)^{N_{\mathrm{fre}}-1}$. The logarithmic scale has been chosen to have a uniform relative resolution so that the low frequencies, which contain most of the energy, are well represented. The starting frequency is typically $f_{\min} = 0.03$–0.04 Hz.

The initial condition was a JONSWAP spectrum [6] with a high value of the peak frequency, giving a small value of the initial energy, of the order of a few cm. The energy balance equation was integrated using a 'fully' implicit scheme (see following section). The integration step was 15 min and the wind speed was chosen to be 18.45 m/s.

In Fig. 1 we show the evolution in time of the one-dimensional frequency spectrum $F(f)$[6] over the first 24 h of the simulation. The evolution of the simulated frequency spectrum is in accord with the results found during

[6] The one-dimensional frequency spectrum is obtained from the two-dimensional frequency-direction spectrum by integration over direction.

Please cite this article in press as: P.A.E.M. Janssen, Progress in ocean wave forecasting, J. Comput. Phys. (2007), doi:10.1016/j.jcp.2007.04.029

the JONSWAP campaign. In particular, in the course of time a considerable downshift of the peak of the spectrum is seen, corresponding with the generation of longer waves, and, in addition a pronounced overshoot of the peak of the spectrum is noted. This latter feature is in agreement with the overshoot phenomenon observed by Barnett and Wilkerson [4]. These authors measured for growing wind waves the evolution in time of the energy of a single wave component. At that time the prevailing wisdom was that there were only two physical processes relevant, namely wind-wave generation and dissipation by white-capping. Hence the expectation was that the energy in a frequency bin would first increase exponentially because of the action of wind (a linear phenomenon) until the waves became so steep that further growth was arrested by white-capping. Surprisingly, rather than observing limit cycle behaviour, after an initial exponential growth phase a pronounced overshoot above the final time saturation limit was found.

In order to better understand the evolution of a gravity wave spectrum we need to study the source functions. To that end, the energy balance for young windsea (duration is 4 h) is shown in Fig. 2, by plotting the directional averages of $S_{\rm in}$, $S_{\rm nl}$, and $S_{\rm ds}$ as function of frequency. As expected from the previous discussions the wind input is always positive, and the dissipation is always negative, while the nonlinear interactions show a three lobe structure of different signs.[7] Therefore, the intermediate frequencies receive energy from the airflow which is transported by the nonlinear interactions towards the high and low frequencies. In the high-frequency range the nonlinear energy flux maintains an equilibrium spectrum which has an f^{-4} shape [52], while in the low-frequency range the nonlinear interactions maintain an 'inverse' energy cascade transferring energy towards the region just below the spectral peak, thereby shifting the peak of the spectrum towards lower frequencies. This frequency downshift is to a large extent determined by the shape and the magnitude of the spectral peak itself. For young windsea, having a narrow peak with a considerable peak enhancement, the rate of downshifting is considerable, while for gentle, old windsea this is much less so. In the course of time the peak of the spectrum gradually shifts towards lower frequencies (as may be seen from Fig. 1) until the peak of the spectrum no longer receives input from the wind because these waves are running faster than the wind. Under these circumstances the waves around the spectral peak are subject to a considerable dissipation so that their steepness reduces. Consequently, because the nonlinear interactions depend on the steepness, the nonlinear transfer is reduced as well, with the result that slowly a quasi-equilibrium spectrum emerges. For old windsea the time scale of downshifting becomes larger than the typical duration of a storm so that for all practical purposes the wind-generated waves evolve towards a steady state.

3. Numerics of the energy balance equation

In this section, numerical aspects of the action balance equation are discussed as they are implemented in the European Centre version of the WAM model (called ECWAM).

It is important to make a distinction between a prognostic part and a diagnostic part of the spectrum. An important reason to introduce a diagnostic part of the spectrum is efficiency: realizing that the high-frequency waves have short time scales the explicit solution of these short waves might require a short time step which may be too expensive. More importantly though, in the high-frequency range another wave breaking process becomes important, which is usually referred to as micro-scale breaking, which is difficult to model in terms of source functions. As already briefly mentioned in the discussion of the nonlinear transfer, nonlinear interactions will set up an energy cascade towards the high-frequencies which results in a quasi-equilibrium spectrum that has an f^{-4} shape. The consequence of this spectral shape is that the local wave steepness increases with increasing frequency. But this cannot continue indefinitely because for a certain frequency the local steepness will hit the breaking limit and consequently micro-scale wave breaking will occur. The corresponding spectrum has an f^{-5} shape [53] which has a local steepness which is independent of the frequency. Therefore, a transition from an f^{-4} to an f^{-5} spectrum is expected, which is in agreement with observational evidence of the high-frequency tail of the wave spectrum.

[7] The nonlinear transfer cannot have a two-lobe structure because the resonant-four wave interactions conserve the two scalar quantities action and energy.

Please cite this article in press as: P.A.E.M. Janssen, Progress in ocean wave forecasting, J. Comput. Phys. (2007), doi:10.1016/j.jcp.2007.04.029

The prognostic part of the spectrum is now obtained by numerically solving the energy balance equation. It has $N_{\rm ang}$ directions and $N_{\rm fre}$ frequencies, where the frequencies are on a logarithmic scale.

Beyond the high-frequency limit $f_{\rm hf}$ of the prognostic region of the spectrum an f^{-5} tail is added with the same directional distribution as the last band of the prognostic region. The diagnostic part of the spectrum is therefore given by

$$F(f,\theta) = F(f_{\rm hf},\theta)\left(\frac{f}{f_{\rm hf}}\right)^{-5} \quad \text{for } f \geqslant f_{\rm hf}. \tag{20}$$

The high-frequency limit is set as

$$f_{\rm hf} = \min\{f_{\max}, 2.5\langle f\rangle_{\rm ws}\}, \tag{21}$$

where $\langle f\rangle_{\rm ws}$ is the mean frequency of the windsea part of the spectrum. A diagnostic tail is added for $f \geqslant f_{\rm hf}$ in order to compute the nonlinear energy transfer in the high-frequency part of the prognostic range and also to compute a number of integral quantities such as occur in the dissipation and wind input source function. Note that the contribution from the diagnostic tail to the total energy is normally small, but quantities such as the mean square slope and the wave-induced stress depend in a sensitive manner on the spectral tail.

The prognostic part of the spectrum is now obtained by numerically solving the energy balance equation. Let us now discuss the different numerical schemes that are used to integrate the source functions and the advective terms of the transport equation.

3.1. Implicit scheme for the source functions

The energy balance equation for the wave spectrum is evaluated in detail up to a high-frequency cut-off $f_{\rm hf}$. The high-frequency relaxation time scales are considerably shorter than the time scales of the energy-containing low-frequency waves, which are of main interest in practical applications. Hence, in the high-frequency region it is sufficient to determine the equilibrium level to which the spectrum adjusts in response to the slowly changing low-frequency waves. Implicit integration schemes whose time step are matched to the evolution of the low-frequency waves meet this requirement automatically: for the low-frequency waves the integration scheme yields the same results as a simple forward integration scheme, while for the high-frequencies the method gives the slowly varying equilibrium spectrum [13,14].

The implicit difference equations (leaving out the advection terms) are given by

$$F_{n+1} = F_n + \Delta t(\alpha S_{n+1} + (1-\alpha)S_n) \tag{22}$$

where Δt is the time step and the index n refers to the time level. The parameter α is a constant. If the source terms depend linearly on F then for a stable numerical scheme α should be at least 1/2. For a linear source term it is straightforward to solve Eq. (22) directly for the spectrum F_{n+1}.

However, none of the source terms are linear. Therefore, a Taylor expansion

$$S_{n+1} = S_n + \frac{\partial S_n}{\partial F}\Delta F \tag{23}$$

is introduced. The functional derivative in (23) can be divided into a diagonal matrix Λ_n and a nondiagonal remainder R_n,

$$\frac{\partial S_n}{\partial F} = \Lambda_n + R_n. \tag{24}$$

Trial computations (cf. [13,14]) indicated that the off-diagonal contributions were generally small for not too large time step. Disregarding these contributions and substitution of (24) and (23) into (22) gives realizing that S may depend on the friction velocity at time level $n+1$,

$$[1 - \alpha\Delta t\Lambda_n(u_*^{n+1})]\Delta F = \Delta t[(1-\alpha)S_n(u_*^n) + \alpha S_n(u_*^{n+1})], \tag{25}$$

where $\Delta F = F_{n+1} - F_n$ is the increment in the spectrum owing to the physics. As a consequence, the increment ΔF becomes

Please cite this article in press as: P.A.E.M. Janssen, Progress in ocean wave forecasting, J. Comput. Phys. (2007), doi:10.1016/j.jcp.2007.04.029

$$\Delta F = \frac{\Delta t[(1-\alpha)S_n(u_*^n) + \alpha S_n(u_*^{n+1})]}{[1 - \alpha \Delta t \Lambda_n(u_*^{n+1})]}. \tag{26}$$

Originally, we took the marginally stable choice $\alpha = 1/2$, however, Hersbach and Janssen [54] noted the occurrence of numerical noise and therefore suggested the use of a fully-implicit scheme with $\alpha = 1$. For this choice of $\alpha = 1$ Eq. (27) becomes

$$\Delta F = \frac{\Delta t S_n(u_*^{n+1})}{1 - \Delta t \Lambda_n(u_*^{n+1})}, \tag{27}$$

which gives a considerable simplification because only the source term with $u_* = u_*^{n+1}$ needs to be evaluated in addition to the diagonal part of its functional derivative.

Nevertheless, in practice, numerical instability is found in the early stages of wave growth. This is either caused by the neglect of the off-diagonal contributions of the functional derivative or more likely by the fact that the solution may not always be close to the attractor of the complete source function. Therefore, a limitation on spectral change needs to be introduced; for details see [54].

3.2. Advective terms

The advective terms in the energy balance equation have been written in the flux form. As an illustration we shall consider the one-dimensional advection equation

$$\frac{\partial F}{\partial t} = -\frac{\partial \Phi}{\partial x}, \tag{28}$$

with flux $\Phi = v_g F$, since the generalization to four-dimensions λ, ϕ, θ and ω is obvious. A number of alternative propagation schemes have been tested by different groups in the past decade. Examples are first-order upwinding schemes, a second order leap frog scheme, semi-Lagrangian schemes, third-order schemes, etc., therefore there exists a considerable amount of experience with discretization of the advection equation. However, none of the schemes give satisfactory results unless special measures are taken. In fact, a propagation scheme with vanishingly small errors would give poor results for sufficiently large propagation times since it would not account for the dispersion associated with the finite resolution of the wave spectrum in frequency and direction (the so-called *Garden-Sprinkler effect*).

In order to explain the Garden-Sprinkler effect, let us study the evolution in space and time of one spectral bin having a width Δf, $\Delta\theta$,

$$\frac{\partial F}{\partial t} + v_g \frac{\partial F}{\partial x} = 0, \tag{29}$$

where we have taken a group speed which is independent of the spatial coordinate x. For the initial condition

$$F(x,0) = f(x) \tag{30}$$

it is straightforward to solve for the evolution of the wave spectrum. The solution becomes

$$F(x,t) = f(x - v_g t) \tag{31}$$

hence the waves with group speed v_g propagate over the surface with a spatial distribution that does not change its shape. Since this is a linear problem, the solution for an arbitrary number of spectral bins is obtained by summation of the solution (31) for different group velocity. Consider the solution for two neighbouring frequency bins and suppose that the two bins have equal spatial distribution of the box type with width Δx, where Δx is the spatial resolution. Clearly, after a finite time τ_s there is a separation of the two pulses which is determined by the difference in group velocity and the spatial width. Assuming that the frequency increment Δf is small, one may use a Taylor expansion of the difference in group velocity and the separation time τ_s becomes

$$\tau_s = \frac{\Delta x}{v_g} \frac{f}{\Delta f} \tag{32}$$

Please cite this article in press as: P.A.E.M. Janssen, Progress in ocean wave forecasting, J. Comput. Phys. (2007), doi:10.1016/j.jcp.2007.04.029

For larger time droplets are formed on the surface, hence the name Garden-Sprinkler effect. In a similar vein, it can be shown that a finite directional resolution $\Delta\theta$ will give rise to the Garden-Sprinkler effect as well. Consider now a basin of length L_x, then the question is of interest under what condition the Garden-Sprinkler effect can be avoided, again using a perfect advection scheme. The answer to this question is straightforward. The travel time τ_t of the waves across the basin is given by $\tau_t = L_x/v_g$. Hence, the Garden-Sprinkler effect can be avoided when the travel time of the waves is less than the separation time τ_s or

$$\frac{\Delta f}{f} < \frac{\Delta x}{L_x}, \tag{33}$$

which amounts for basins of a global scale, say $L_x \simeq 10^4$ km, and a spatial resolution $\Delta x \simeq 50$ km to a very stringent condition on the frequency resolution, as $\Delta f/f < 0.005$.

It is emphasized that for a continuous spectrum the Garden-Sprinkler effect will not occur and therefore in a discrete model measures have to be taken to avoid it. The Garden-Sprinkler effect can be avoided by realizing that inside one bin the group speed varies with frequency. Working out the consequences [55] one finds that in good approximation the energy density F_n in a bin Δf_n satisfies an advection diffusion equation of the type

$$\frac{\partial F_n}{\partial t} + v_{g,n}\frac{\partial F_n}{\partial x} = D\frac{\partial^2 F_n}{\partial x^2},$$

where $v_{g,n}$ is the mean group speed of the bin and the diffusion coefficient D is proportional to the age (time!) of the wave packets. This gives, as expected from dispersion, a linear spreading rate. However, it is an expensive solution because the age of each spectral bin is required.

The compromise now is to use schemes with a *constant* diffusion coefficient. This explains why a first-order upwinding scheme is so successful, despite the fact that it is only first order accurate and is highly diffusive having a numerical diffusion coefficient $D \simeq (\Delta x)^2/\Delta t$ (with Δt the time step).

To summarize the discussion, we have chosen the first-order upwinding scheme because of its simplicity, because it requires less memory and computer time and because in practice it gives reasonable results. Remark that there are other error sources, e.g. the quality of the forcing wind fields, which are dominating the error budget of a wave prediction system (for a more detailed discussion of this see Section 4). Applied to the simple advection scheme in flux form (28) one obtains the following discretization, where for the definition of grid points we refer to Fig. 3. The rate of change of the spectrum ΔF_j in the jth grid point is given by

$$\Delta F_j = -\frac{\Delta t}{\Delta x}(\Phi_{j+1/2} - \Phi_{j-1/2}), \tag{34}$$

where Δx is the grid spacing and Δt the propagation time step, and

$$\Phi_{j+1/2} = \frac{1}{2}[u_j + |u_j|]F_j + \frac{1}{2}[u_j - |u_j|]F_{j+1}, \tag{35}$$

where $u_j = 0.5(v_{g,j} + v_{g,j+1})$ is the mean group velocity and the flux at $j - 1/2$ is obtained from (35) by replacing $j + 1/2$ with $j - 1/2$. The absolute values of the mean speeds arise because of the upwinding scheme. For example, for flow going from the left to the right the speeds are positive and, as a consequence, the evaluation of the gradient of the flux involves the spectra at grid points $j - 1$ and j.

Finally, it is important to remark that the first-order upwinding scheme suffers from numerical instabilities when the time step is so large that the so-called Courant–Friedrichs–Levy (CFL) criterion is violated. The one-dimensional upwinding scheme is stable provided

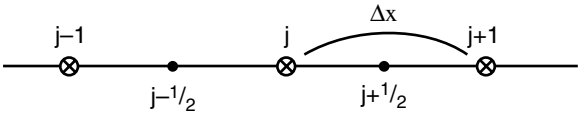

Fig. 3. Definition of grid points for first-order upwinding scheme.

Please cite this article in press as: P.A.E.M. Janssen, Progress in ocean wave forecasting, J. Comput. Phys. (2007), doi:10.1016/j.jcp.2007.04.029

675 $$v_g < \frac{\Delta x}{\Delta t},$$

676 in other words, wave groups are only allowed to travel during one time step at most one grid length. The CFL
677 criterion may become critical in particular near the poles when spherical coordinates are used: when moving
678 towards the poles, the actual distance in the longitudinal direction decreases. Clearly, the closer one moves to
679 the poles, the more likely it becomes that the CFL criterion is violated. This problem is solved by choosing an
680 irregular spherical grid in such a way that the longitudinal distance is fixed to its value at the equator. The
681 advection scheme is still formulated in terms of normal spherical coordinates but the gradient in the longitu-
682 dinal fluxes is evaluated by linear interpolation of the fluxes from the closest neighbours.The additional advan-
683 tage of the use of an irregular spherical grid is a reduction in the total number of grid points by 30%, giving a
684 substantial reduction in the number of computations.

685 ## 4. Validation of wave forecasts

686 ECMWF introduced the third-generation WAM model in operations on the 21st of June 1992. Since that
687 date there has been a continuous effort to improve the skill of the wave forecasting system. While in 1992 the
688 spatial resolution of the wave model was 330 km, over the years resolution has increased quite dramatically
689 and presently the global version of the model runs on a 40 km grid. This increase in resolution was only pos-
690 sible after a large effort in upgrading the wave model software from its original version which ran very effi-
691 ciently on vector machines. For example, in order to improve efficiency, options for macrotasking (later
692 replaced by open MP directives) and massive parallel processing were introduced. In addition, the software
693 now fully complies with Fortran 90 standards. The advantage of this is that only one executable is needed
694 for all the relevant applications, such as the deterministic 10-day forecast with resolution of 40 km, the ensem-
695 ble forecast with a resolution of 100 km and the limited area forecasts with a resolution of 28 km. The same
696 executable can also be run as a one grid point model, which is convenient when testing changes in physics for
697 example.
698 One of the reasons to develop a third-generation wave model was the prospect of the availability of satellite
699 measurements of wave parameters and the surface wind field on a global scale. On the one hand, this provided
700 a unique opportunity to validate wave models and atmospheric models, on the other hand these data could be
701 used to generate a more optimal initial condition by means of a process that is called the analysis. In the sum-
702 mer of 1991 ESA launched the ERS-1 satellite which carried on board three instruments which measured
703 information relevant for ocean waves. A scatterometer measured the surface wind field in a fairly wide swath,
704 an altimeter measured the significant wave height along a nadir track every 7 km, while a synthetic aperture
705 radar (SAR) provided information on the two-dimensional energy distribution of the long waves, every
706 200 km. Eventually, all these data sources found their way into the data assimilation scheme of the atmo-
707 spheric model and the ocean wave model.
708 Finally, a number of model changes were introduced in the 15 year period. We mention the two-way inter-
709 action of wind and waves, effects of unresolved bathymetry, and a new formulation of the dissipation source
710 function. It should be clear that such a large programme of change can only be successful after an extensive
711 and careful verification effort.
712 An important element of any operational forecasting system is its verification against observations. The
713 main verification activities are concentrated on the deterministic medium-range forecast. Analyzed and fore-
714 cast parameters such as significant wave height and mean period are routinely verified against independent
715 buoy data. A number of operational centres involved in ocean-wave forecasting take part in a project to assess
716 forecast performance against buoy data [56]. However, buoy data are usually only available near coastal areas
717 in the Northern Hemisphere. In order to assess the global performance of the wave prediction system we com-
718 pare first-guess wave heights against Altimeter wave heights, and we compare forecast wave height against the
719 verifying analysis. Furthermore, the quality of the wave forecast depends to a considerable extent on the qual-
720 ity of the forcing wind fields. For this reason, analysed surface winds are validated against independent Altim-
721 eter wind speed observations while forecast wind speed is validated against the verifying analysis. An overview
722 of these activities is given in [57] and in [58].

Please cite this article in press as: P.A.E.M. Janssen, Progress in ocean wave forecasting, J. Comput. Phys. (2007), doi:10.1016/j.jcp.2007.04.029

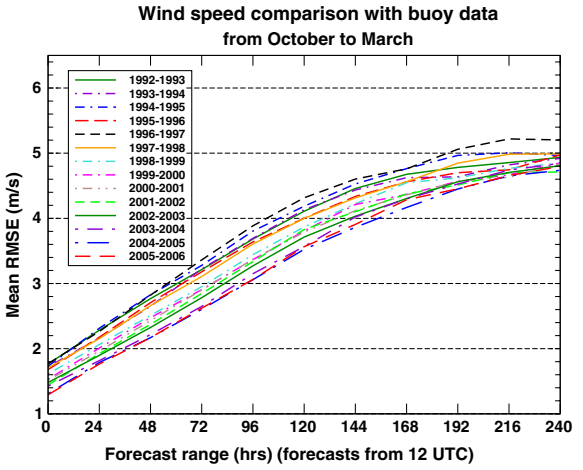

Fig. 4. Verification of analyzed and forecast surface wind speeds against buoy observations.

Here, we illustrate progress in wave forecasting by means of a verification of forecast winds and wave height against buoy observations. We also validate modelled analyzed spectra against wave spectral data. Note that buoy observations of significant wave height and of the wave spectrum are independent as they are not assimilated in our analysis scheme. Observations of the surface wind are, however, assimilated in the atmospheric analysis system, so that wind speed analysis and buoy observations are not independent. During the forecast, the correlation between observed and forecast wind diminishes very quickly, and after day one in the forecast it is safe to assume that observations of wind are independent of the model. In Fig. 4 we show the results of the verification of analyzed and forecast wind speed against buoy data for a number of winter seasons, here defined as the period from October to March, starting in 1992 and ending in 2005. The overall trend is that there is a clear reduction in modelled wind error over the years. Considering now the forecast wave height verification against buoy data in Fig. 5 there seems to be even a stronger trend of improvement in forecast wave height, in particular in the medium range around day 5. The present-day forecast error at day 6 of the forecast is smaller in magnitude than the day 4 forecast error 15 years ago, suggesting an improvement in skill of more than 2 days.

The stronger trend in improvement in forecast wave height in the medium range[8] is a reflection of the sensitive dependence of the significant wave height on the forcing wind field. To illustrate this point, it is noted that dimensional considerations show that in equilibrium conditions (but note that for big storms we hardly ever reach equilibrium) the significant wave height H_S depends on the square of the wind speed at 10 m height above the sea surface,

$$H_S = \beta U_{10}^2/g, \quad \beta \simeq 0.22, \tag{36}$$

therefore a 10% error in wind speed already gives a 20% error in wave height. Note that the statistical results here refer to the bulk of the data, with an average wind speed of 7 m/s. For such low wind speeds the sea state is almost always in equilibrium [57]. Figs. 4 and 5 do suggest that an important component of the wave height error is the surface wind speed error. This is in agreement with the practical experience of many wave modellers and forecasters. In fact, by redoing wave height analyses with the most recent version of our wave prediction model using ECMWF analysed winds from 1997 we have been able to estimate that our wave model improvements contribute about 25% to the improvement in accuracy of the wave height analysis shown in Fig. 5. Hence, the increased accuracy of the driving wind field is the main reason for the improved accuracy of the analysed wave height. Because of the sensitive dependence of wave model results on the quality of the surface wind field, ocean-wave information can give benefits for atmospheric modelling. Wave results have

[8] There is an even stronger trend of improvement at initial time, but this is partly caused by the fact that the buoy windspeeds have been used in the atmospheric analysis, thus constraining the analysed wind speed.

Please cite this article in press as: P.A.E.M. Janssen, Progress in ocean wave forecasting, J. Comput. Phys. (2007), doi:10.1016/j.jcp.2007.04.029

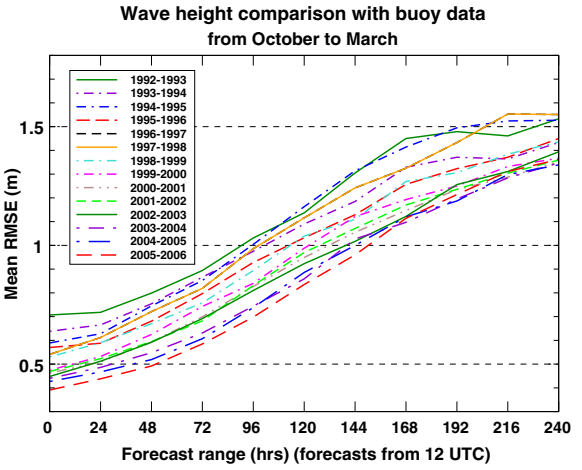

Fig. 5. Verification of analyzed and forecast significant wave height against buoy observations.

already been used to diagnose planetary boundary problems and to study overactivity of the atmospheric model [59].

The discussion on verification is closed by presenting a relatively new diagnostic tool which enables to study problems in the modelled spectral shape. This is now opportune because a consequence of the large improve-

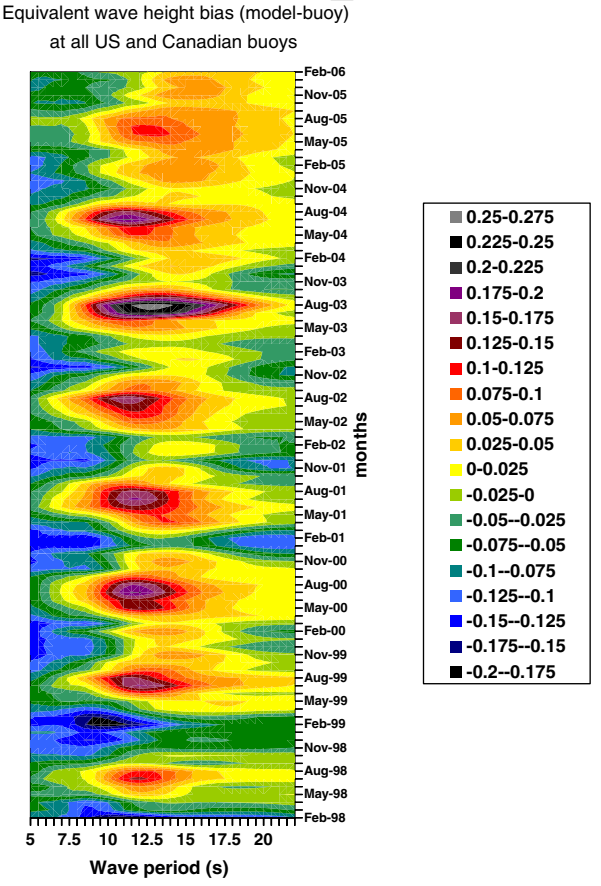

Fig. 6. Spectral bias (model-buoy) at all US and Canadian buoys for the period February 1998 until February 2006.

Please cite this article in press as: P.A.E.M. Janssen, Progress in ocean wave forecasting, J. Comput. Phys. (2007), doi:10.1016/j.jcp.2007.04.029

ments in the forcing wind fields is that it is nowadays more straightforward to identify (systematic) errors in the wave model. This tool was first introduced by Voorrips et al. [60] in a study to validate SAR and wave model frequency spectra against buoy spectra. One simply determines for each frequency, hence wave period the wave variance from the modelled and observed frequency spectra in a period bin of, say, two seconds and one obtains the 'equivalent' wave height by the usual definition. The resulting period dependent bias is then plotted as a function of time. In Fig. 6 (see also [61]) an example is given involving all American and Canadian one-dimensional frequency spectra over the period of February 1998 until February 2006. In the range of 10–15 s there is up to 2003, a clear seasonal dependence of the 'equivalent' wave height bias, being large in the summer time and vanishingly small in the winter time.

It turns out that these large positive biases are related to swell events generated by the storms in the Southern Hemisphere winter time. It would be tempting to speculate on the causes of the overestimate by the wave model. An obvious candidate would be the dissipation source function, because this source term is the least well understood. Another candidate is the representation of unresolved islands and atolls. A closer inspection of the verification results revealed that the main problem occurs in the Pacific ocean and not in the Atlantic (not shown). An important difference between the Pacific and the Atlantic ocean is that in the equatorial region of the Pacific there are a vast number of small islands and atolls which are not resolved by the present operational resolution of the wave model. Although these islands are small, they nevertheless block considerable amounts of low-frequency wave energy [62]. Therefore, using a high resolution global topography of 2 min, Bidlot (private communication, 2003) determined a wavenumber dependent blocking factor. This change was introduced operationally in February 2004 and, as can be seen from Fig. 6, gave a substantial reduction of the bias in the Summer of 2004. Nevertheless, it did not disappear completely.

In March 2005 a new version of the dissipation source function was introduced, which used an alternative definition of the integral parameters, such as mean frequency, in the expression for the dissipation. The new definition is given in Eq. (16). As can be seen in Fig. 6, this change had a further beneficial impact as in the Summer of 2005 there is virtually no bias anymore in the range of 10–15 s.

5. A new development

The energy balance equation gives a description of the mean state, as characterized by the wavenumber spectrum, for a box, $\Delta x \times \Delta y$ wide, surrounding a grid point located at $\mathbf{x}$. The question is of vital interest whether one can get information on the distribution of, for example, the significant wave height around the average grid box value. In lowest order, the probability distribution function (pdf) for the surface elevation is a Gaussian, corresponding to the case of linear waves. However, dynamical effects of finite amplitude will change the shape of the pdf, and these changes can be calculated. This results in valuable information on extreme sea states.

Recall that the nonlinear four-wave interactions have been obtained by closing the infinite hierarchy of moment equations with the statistical assumption that the system remains close to Gaussian. However, finite deviations from the normal distribution are required in order to get a meaningful evolution of the spectrum, which, by the way, is given by the Hasselmann equation (14). The deviations from Normality contain, however, useful statistical information in itself. For example, one may determine interesting parameters such as the skewness and the kurtosis of the pdf of the surface elevation. Deviations from Normality are most conveniently expressed by means of the kurtosis,

$$C_4 = <\eta^4> / 3 <\eta^2>^2 - 1. \tag{37}$$

For a Normal distribution, C_4 vanishes. Then, consistent with the evolution equation for the four-wave interactions the kurtosis becomes

$$C_4 = \frac{4}{g^2 m_0^2} \int \mathrm{d}\mathbf{k}_{1,2,3,4} T_{1,2,3,4} \delta_{1+2-3-4} (\omega_1 \omega_2 \omega_3 \omega_4)^{\frac{1}{2}} \frac{N_1 N_2 N_3}{\Delta\omega}, \tag{38}$$

where $\Delta\omega = \omega_1 + \omega_2 - \omega_3 - \omega_4$. Hence, the kurtosis is determined by both resonant and non-resonant interactions and depends on the action density to the third power. The exact expression for the kurtosis, being a six-dimensional integral, is too time consuming to evaluate. Therefore, for operational applications an efficient

Please cite this article in press as: P.A.E.M. Janssen, Progress in ocean wave forecasting, J. Comput. Phys. (2007), doi:10.1016/j.jcp.2007.04.029

parametrization is required. As a first step one could follow the approach reported in [63], which relates the kurtosis to the Benjamin–Feir index (BFI). This is a spectral parameter which equals the ratio of nonlinearity to coherency of the nonlinear wave field, and measures the efficiency of the energy transfer between wave components of the spectrum. For large BFI, which corresponds to a strong nonlinear, coherent wave field, there is a considerable energy transfer possible resulting in focussing of energy in space and time and consequently in the possibility of extreme sea states such as freak waves.

The BFI is defined as

$$\mathrm{BFI} = \epsilon\sqrt{2}/\Delta, \tag{39}$$

where $\epsilon = (k_\mathrm{p}^2\langle\eta^2\rangle)^{1/2}$ is an integral measure of wave steepness (here, $\langle\eta^2\rangle = m_0$ is the wave variance and k_p is the peak wave number), while $\Delta = \sigma_\omega/\omega_\mathrm{p}$ is the relative width of the frequency spectrum and is a measure for the coherency of the wave field. Let us restrict our attention to spectra that are completely characterized by the zero moment m_0 and by the width in frequency direction (σ_ω) and in angular direction (σ_θ). Scaling considerations applied to Eq. (38) then suggest that the kurtosis C_4 depends on the square of the BFI,

$$C_4 = \Gamma(\sigma_\theta/\sigma_\omega) \times \mathrm{BFI}^2, \tag{40}$$

where the function Γ may be evaluated analytically under special circumstances. For example, for uni-directional waves (with $\sigma_\theta = 0$), and Gaussian spectra one finds $\Gamma(0) = \pi/3\sqrt{3}$. In October 2003 ECMWF introduced a first version of an extreme wave detection system based on Eq. (40) for uni-directional waves. However, effects of finite directional width are important as well, because these will reduce the coherency of the nonlinear system, thus reducing the probability on extreme events. Presently work is under way to extend this system to two-dimensional propagation.

The theoretical approach regarding spectral evolution and the corresponding statistical properties of the sea surface have been validated by means of Monte Carlo simulations of the deterministic evolution equations (12) [47]. In addition, the theoretical approach compares favourably with wave tank observations obtained by Onorato et al. [64]. This is shown in Fig. 7 which gives the probability $P_\mathrm{H}(h)$ that instantaneous wave height exceeds h times the significant wave height H_S, according to observations, nonlinear theory [63] and according to linear theory (Rayleigh distribution). Note that the theoretical distribution assumes a very simple form, as

$$P_\mathrm{H}(h) = \mathrm{e}^{-2h^2}[1 + C_4 B_\mathrm{H}(h)], \quad B_\mathrm{H}(h) = 2h^2(h^2 - 1). \tag{41}$$

As can be seen from Fig. 7 and from Eq. (41), for positive kurtosis there are considerable increases in the probability of extreme sea states, and, indeed, from the observed time series in the tank a number of freak waves were visible.

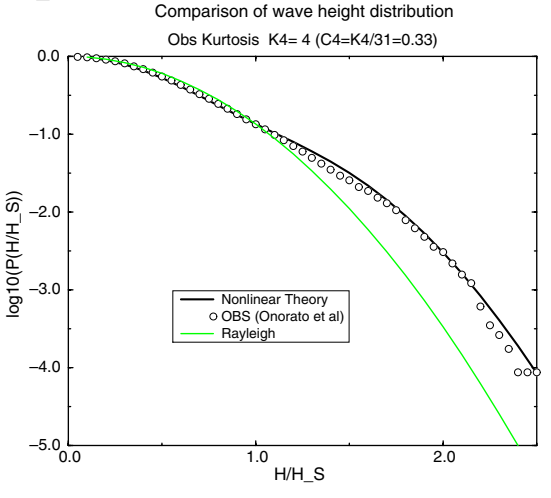

Fig. 7. Comparison of theoretical and observed [64] wave height distribution. For reference, the linear Rayleigh result is shown as well.

Please cite this article in press as: P.A.E.M. Janssen, Progress in ocean wave forecasting, J. Comput. Phys. (2007), doi:10.1016/j.jcp.2007.04.029

This new development has already given promising results. But it should be clear that there is still a lot of work to be done before it becomes a reliable tool for the prediction of extreme events such as freak waves. First, we need to obtain an efficient, general parametrization of the expression for the kurtosis parameter. Second, the approach needs to be extended to shallow waters [42]. Finally, we need to validate these predictions in the field, which is a difficult task as freak wave events only occur rarely.

6. Conclusions

It is indeed true that in the past 50 year or so we have seen massive improvements in our ability to forecast ocean waves. The reasons for these improvements have been discussed to some extent in this paper: a more realistic modelling of the dynamics of ocean waves, vast improvements in atmospheric modelling resulting in accurate surface winds, a large increase in observations of the sea state and the atmosphere, notably provided by satellites, etc.

It is justified to ask the question whether there is still a need for further wave-model development. There are most certainly definite reasons for this and they derive, as it should, from a number of applications in which the wave spectrum plays an important role. In our field, applications are an important driver for new developments, and in particular, *new* applications will no doubt expose weaknesses of the present wave forecasting systems.

Just recently we have seen rapid progress in the understanding of the mechanisms behind the generation of extreme sea states such as freak waves. Prediction of enhanced probabilities of extreme events would be of tremendous benefit to the marine world, but clearly an accurate prediction of the detailed low-frequency part of the wave spectrum is of utmost importance. This capability of wind-wave forecasting systems is, as yet, unproven. Furthermore, more research into the relation between spectral shape and the occurrence of extreme states is highly desirable.

On the other hand, knowledge of the high-frequency part of the wave spectrum is important in all remote-sensing applications that depend to some extent on properties of the sea surface. We mention instruments such as the Altimeter, the Scatterometer, SSM/I, ATOVS, in short, any instrument that involves aspects of specular reflection. In fact, the ocean surface albedo depends in a straightforward manner on properties of the slope spectrum. Also, knowledge of the high-frequency spectrum is important in order to determine the air–sea momentum exchange, and as a consequence it is also important for the exchange of 'passive' scalars such as CO_2. In this paper we have presented a parametrization of the high-frequency spectrum which may be regarded as a good first-guess. Nevertheless, the actual spectral shape is not well understood and a significant amount of experimental and theoretical work is still needed to obtain a convincing and working model for the high-frequencies.

Finally, we have indicated in this paper that ocean waves play a role in the air-sea momentum transfer. Once the waves break they dump their energy into the ocean column, thereby directly feeding the large scale ocean circulation. Also, ocean waves are affected by surface currents, hence it makes sense to couple an ocean wave model and an ocean circulation as well. The end result is one model for the geosphere. At ECMWF, the first steps towards such a model have already been taken and this model is used in our seasonal forecasting system.

Acknowledgement

The author acknowledges useful and stimulating discussions with Saleh Abdalla, Jean Bidlot and Hans Hersbach.

References

[1] H. Jeffreys, On the formation of waves by wind, Proc. Roy. Soc. A107 (1924) 189–206.
[2] H. Jeffreys, On the formation of waves by wind. II, Proc. Roy. Soc. A110 (1925) 341–347.
[3] J.W. Miles, On the generation of surface waves by shear flows, J. Fluid Mech. 3 (1957) 185–204.
[4] T.P. Barnett, J.C. Wilkerson, On the generation of ocean wind waves as inferred from airborne measurements of fetch-limited spectra, J. Mar. Res. 25 (1967) 292–328.

Please cite this article in press as: P.A.E.M. Janssen, Progress in ocean wave forecasting, J. Comput. Phys. (2007), doi:10.1016/j.jcp.2007.04.029

[5] H. Mitsuyasu, R. Nakayama, T. Komori, Observations of the wind and waves in Hakata bay, Rep. Res. Inst. Appl. Mech., Kyushu Univ. 19 (1971) 37–74.
[6] K. Hasselmann, T.P. Barnett, E. Bouws, H. Carlson, D.E. Cartwright, K. Enke, J.A. Ewing, H. Gienapp, D.E. Hasselmann, P. Kruseman, A. Meerburg, P. Müller, D.J. Olbers, K. Richter, W. Sell, H. Walden, Measurements of wind-wave growth and swell decay during the Joint North Sea Wave Project (JONSWAP), Dtsch. Hydrogr. Z. Suppl. A 8 (12) (1973), 95pp.
[7] R.L. Snyder, F.W. Dobson, J.A. Elliott, R.B. Long, Array measurements of atmospheric pressure fluctuations above surface gravity waves, J. Fluid Mech. 102 (1981) 1–59.
[8] D.E. Hasselmann, J. Bösenberg, Field measurements of wave-induced pressure over wind sea and swell, J. Fluid Mech. 230 (1991) 391–428.
[9] J.H. Allender, T.P. Barnett, L. Bertotti, J. Bruinsma, V.J. Cardone, L. Cavaleri, J. Ephraums, B. Golding, A. Greenwood, J. Guddal, H. Günther, K. Hasselmann, S. Hasselmann, P. Joseph, S. Kawai, G.J. Komen, L. Lawson, H. Linné, R.B. Long, M. Lybanon, E. Maeland, W. Rosenthal, Y. Toba, T. Uji, W.J.P. de Voogt, A. Greenwood, J. Guddal, H. Günther, K. Hasselmann, S. Hasselmann, P. Joseph, S. Kawai, G.J. Komen, L. Lawson, H. Linné, R.B. Long, M. Lybanon, E. Maeland, W. Rosenthal, Y. Toba, T. Uji, W.J.P. de Voogt, A. Greenwood, J. Guddal, H. Günther, K. Hasselmann, S. Hasselmann, P. Joseph, S. Kawai, G.J. Komen, L. Lawson, H. Linné, R.B. Long, M. Lybanon, E. Maeland, W. Rosenthal, Y. Toba, T. Uji, W.J.P. de Voogt, Sea wave modeling project (SWAMP). An intercomparison study of wind wave predictions models, part 1: principal results and conclusions, in: Ocean Wave Modeling, Plenum Press, New York, 1985, 256pp.
[10] G.J. Komen, K. Hasselmann, S. Hasselmann, On the existence of a fully developed windsea spectrum, J. Phys. Oceanogr. 14 (1984) 1271–1285.
[11] W.J. Pierson Jr., L. Moskowitz, A proposed spectral form for fully developed wind seas based on the similarity theory of S.A. Kitaigorodskii, J. Geophys. Res. 69 (1964) 5181.
[12] S. Hasselmann, K. Hasselmann, J.H. Allender, T.P. Barnett, Computations and parameterizations of the nonlinear energy transfer in a gravity wave spectrum, part 2: parameterizations of the nonlinear energy transfer for application in wave models, J. Phys. Oceanogr. 15 (1985) 1378–1391.
[13] S. Hasselmann, K. Hasselmann, E. Bauer, P.A.E.M. Janssen, G.J. Komen, L. Bertotti, P. Lionello, A. Guillaume, V.C. Cardone, J.A. Greenwood, M. Reistad, L. Zambresky, J.A. Ewing, WAMDI group, The WAM model – a third generation ocean wave prediction model, J. Phys. Oceanogr. 18 (1988) 1775–1810.
[14] G.J. Komen, L. Cavaleri, M. Donelan, K. Hasselmann, S. Hasselmann, P.A.E.M. Janssen, Dynamics and Modelling of Ocean waves, Cambridge University Press, Cambridge, UK, 1994.
[15] H.L. Tolman, D.V. Chalikov, Source terms in a third-generation wind wave model, J. Phys. Oceanogr. 26 (1996) 2497–2518.
[16] K. Ueno, N. Kohno, The development of the third generation model MRI-III for operational use, in: Proceedings of the Eighth International Workshop on Wave Hindcasting and Forecasting G2, 2004, pp. 1–7.
[17] N. Booij, R.C. Ris, L.H. Holthuijsen, A third generation model for coastal regions. Part I: model description and validation, J. Geophys. Res. 104 (No. C4) (1999) 7649–7666.
[18] H.U. Sverdrup, W.H. Munk, Wind Sea and Swell: Theory of Relations for Forecasting, H.O. Pub. 601, US Navy Hydrographic Office, Washington, DC, 1947, 44pp.
[19] P. Groen, R. Dorrestein, Zeegolven, Staatsdrukkerij, 's-Gravenhage, 1976, 124pp. 3e herz. druk.
[20] W.J. Pierson, G. Neumann, R.W. James, Practical Methods for Observing and Forecasting Ocean Waves by Means of Wave Spectra and Statistics, H.O. Pub 603, US Navy Hydrographic Office, 1955.
[21] R. Gelci, H. Cazalé, J. Vassal, Prévision de la houle. La méthode des densités spectroangulaires, Inform. Comité Central Océanogr. Etude Côtes 9 (1957) 416–435.
[22] G.B. Whitham, Linear and Nonlinear Waves, Wiley, New York, 1974, 636p.
[23] J.C. Luke, A variational principle for a fluid with a free surface, J. Fluid Mech. 27 (1967) 395–397.
[24] V.E. Zakharov, Stability of periodic waves of finite amplitude on the surface of a deep fluid, J. Appl. Mech. Technol. Phys. 9 (1968) 190–194.
[25] J. Willebrand, Energy transport in a nonlinear and inhomogeneous random gravity wave field, J. Fluid Mech. 70 (1975) 113–126.
[26] P.A.E.M. Janssen, The Interaction of Ocean Waves and Wind, Cambridge University Press, Cambridge, UK, 2004, 300+viii pp.
[27] P.A.E.M. Janssen, Wave-induced stress and the drag of air flow over sea waves, J. Phys. Oceanogr. 19 (1989) 745–754.
[28] K. Hasselmann, On the spectral dissipation of ocean waves due to whitecapping, Boundary Layer Meteorol. 6 (1974) 107–127.
[29] P. Sullivan, J. McWilliams, C.-H. Moeng, Simulation of turbulent flow over idealized water waves, J. Fluid Mech. 404 (2000) 47–85.
[30] T.S. Hristov, S.D. Miller, C.A. Friehe, Dynamical coupling of wind and ocean waves through wave-induced air flow, Nature 442 (2003) 55–58.
[31] M.A. Donelan, The dependence of the aerodynamic drag coefficient on wave parameters, in: Proceedings of the First International Conference on Meteorological and Air/sea Interaction of the Coastal Zone, American Meteorological Society, Boston, MA, 1982, pp. 381–387.
[32] S.D. Smith, R.J. Anderson, W.A. Oost, C. Kraan, N. Maat, J. DeCosmo, K.B. Katsaros, K.L. Davidson, K. Bumke, L. Hasse, H.M. Chadwick, Sea surface wind stress and drag coefficients: the HEXOS results, Boundary Layer Meteorol. 60 (1992) 109–142.
[33] W.M. Drennan, K.K. Kahma, M.A. Donelan, On momentum flux and velocity spectra over waves, Bound.-Layer Meteorol. 92 (1999) 489–515.
[34] W.A. Oost, G.J. Komen, C.M.J. Jacobs, C. van Oort, New evidence for a relation between wind stress and wave age from measurements during ASGAMAGE, Bound.-Layer Meteorol. 103 (2002) 409–438.
[35] G.G. Stokes, On the theory of oscillatory waves, Trans. Camb. Phil. Soc. 8 (1847) 441–455.

[36] T. Levi-Cevita, Determination rigoureuse des ondes permanente d'ampleur finie, Math. Ann. 93 (1925) 264–314.
[37] M.J. Lighthill, Contributions to the theory of waves in non-linear dispersive systems, J. Inst. Math. Appl. 1 (1965) 269–306.
[38] T.B. Benjamin, J.E. Feir, The disintegration of wave trains on deep water. Part I. Theory, J. Fluid Mech. 27 (1967) 417–430.
[39] S. Yu Annenkov, V.I. Shrira, On the predictability of evolution of surface gravity and gravity-capillary waves, Physica D 152–153 (2001) 665–675.
[40] V.P. Krasitskii, On reduced equations in the Hamiltonian theory of weakly nonlinear surface waves, J. Fluid Mech. 272 (1994) 1–20.
[41] D.R. Crawford, B.M. Lake, P.G. Saffman, H.C. Yuen, Stability of weakly nonlinear deep-water waves in two and three dimensions, J. Fluid Mech. 105 (1981) 177–191.
[42] P.A.E.M. Janssen, M. Onorato, The shallow water limit of the Zakharov Equation and consequences for wave prediction, J. Phys. Oceanogr., in press.
[43] K. Hasselmann, On the non-linear energy transfer in a gravity-wave spectrum, part 1: general theory, J. Fluid Mech. 12 (1962) 481.
[44] L.F. McGoldrick, O.M. Phillips, N. Huang, T. Hodgson, Measurements on resonant wave interactions, J. Fluid Mech. 25 (1966) 437.
[45] O.M. Phillips, The dynamics of unsteady gravity waves of finite amplitude, part 1, J. Fluid Mech. 9 (1960) 193–217.
[46] M. Tanaka, Verification of Hasselmann's energy transfer among surface gravity waves by direct numerical simulation of primitive equations, J. Fluid Mech. 444 (2001) 199–221.
[47] P.A.E.M. Janssen, Nonlinear Four-wave interactions and freak waves, J. Phys. Oceanogr. 33 (2003) 863–884.
[48] I.R. Young, A.V. Babanin, Spectral distribution of energy dissipation of wind-generated waves due to dominant wave breaking, J. Phys. Oceanogr. 36 (2006) 376–394.
[49] J.A. Battjes, J.P.F.M. Janssen, Energy loss and set-up due to breaking of random waves, in: Proceedings of the 16th International Conference on Coastal Engineering, American Society of Civil Engineers, Hamburg, Germany, 1978, pp. 569–578.
[50] C. Kraan, W.A. Oost, P.A.E.M. Janssen, Wave energy dissipation by whitecaps, J. Atmos. Oceanic Technol. 13 (1996) 262–267.
[51] C. Lafon, J. Piazzola, P. Forget, O. Le Calve, S. Despiau, Analysis of the variation of the whitecap fraction as measured in a coastal zone, Bound.-Layer Meteor. 111 (2004) 339–360.
[52] V.E. Zakharov, N.N. Filonenko, Energy spectrum for stochastic oscillations of the surface of a liquid, Sov. Phys. Doklady 11 (1967) 881.
[53] O.M. Phillips, The equilibrium range in the spectrum of wind-generated water waves, J. Fluid Mech. 4 (1958) 426–434.
[54] H. Hersbach, P.A.E.M. Janssen, Improvement of the short fetch behavior in the Wave Ocean model (WAM), J. Atm. Oceanic Technol. 16 (1999) 884–892.
[55] N. Booij, L.H. Holthuijsen, Propagation of ocean waves in discrete spectral wave models, J. Comp. Phys. 68 (1987) 307–326.
[56] J.-R. Bidlot, D.J. Holmes, P.A. Wittmann, R. Lalbeharry, H.S. Chen, Intercomparison of the performance of operational ocean wave forecasting systems with buoy data, Weather Forecast. 17 (2002) 287–310.
[57] P.A.E.M. Janssen, B. Hansen, J.-R. Bidlot, Verification of the ECMWF wave forecasting system against buoy and altimeter data, Weather Forecast. 12 (1997) 763–784.
[58] P.A.E.M. Janssen, J. Bidlot, B. Hansen, Diagnosis of the ECMWF ocean-wave forecasting system, ECMWF Techn. Memorandum 318 (2000).
[59] P.A.E.M. Janssen, A.C.M. Beljaars, A. Simmons, P. Viterbo, On the determination of surface stresses in an atmospheric model, Mon. Weather Rev. 120 (1992) 2977–2985.
[60] A.C. Voorrips, C. Mastenbroek, B. Hansen, Validation of two algorithms to retrieve ocean wave spectra from ERS synthetic aperture radar, J. Geophys. Res. 106 (No. C8) (2001) 16, 825–16,840.
[61] J.-R Bidlot, P.A.E.M Janssen, S. Abdalla, On the importance of spectral wave observations in the continued development of global wave models, in: Proceedings of the Fifth International Symposium on Ocean Wave Measurement and Analysis WAVES2005: 3rd–7th July 2005, Madrid, Spain.
[62] H.L. Tolman, Treatment of unresolved islands and ice in wind wave models, Ocean Modell. 5 (2003) 219–231.
[63] N. Mori, P.A.E.M. Janssen, On kurtosis and occurrence probability of freak waves, J. Phys. Oceanogr. 36 (2006) 1471–1483.
[64] M. Onorato, R. Osborne, M. Serio, L. Cavaleri, Modulational instability and non-Gaussian statistics in experimental random water-wave trains, Phys. Fluids 17 (2005) 078101.

Please cite this article in press as: P.A.E.M. Janssen, Progress in ocean wave forecasting, J. Comput. Phys. (2007), doi:10.1016/j.jcp.2007.04.029